Journal of Hazardous Materials 452 (2023) 131247

Contents lists available at ScienceDirect

Journal of Hazardous Materials

journal homepage: www.elsevier.com/locate/jhazmat

A carboxyl-functionalized covalent organic polymer for the efficient adsorption of saxitoxin

Tianxing Wang [a,b], Soraia P.S. Fernandes [a,c], Joana Araújo [a], Xiaoxi Li [b], Laura M. Salonen [d,e,**], Begoña Espiña [a,*]

[a] International Iberian Nanotechnology Laboratory (INL), Avenida Mestre José Veiga, 4715-330 Braga, Portugal
[b] Ministry of Education Engineering Research Center of Starch and Protein Processing, Guangdong Province Key Laboratory for Green Processing of Natural Products and Product Safety, School of Food Science and Engineering, South China University of Technology, Guangzhou 510640, China
[c] Associate Laboratory for Green Chemistry-Network of Chemistry and Technology (LAQV-REQUIMTE), Department of Chemistry, University of Aveiro, Campus Universitário de Santiago, 3810-193 Aveiro, Portugal
[d] CINBIO, Universidade de Vigo, Department of Organic Chemistry, 36310 Vigo, Spain
[e] Nanochemistry Research Group, International Iberian Nanotechnology Laboratory, Braga 4715-330, Portugal

HIGHLIGHTS

- Covalent organic polymer TpPa-COOH for the efficient adsorption of saxitoxin (STX).
- Fast adsorption of STX with equilibrium reached within 1 h.
- Calculated maximum adsorption capacity of 5.69 mg g^{-1} outperforms reported materials.
- Good reusability and high recovery rates for STX in natural freshwater.

GRAPHICAL ABSTRACT

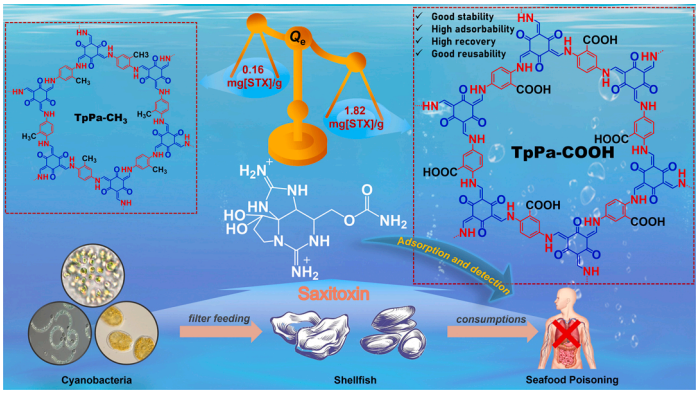

ARTICLE INFO

Editor: Arturo J. Hernandez-Maldonado

Keywords:
Saxitoxin
Covalent organic polymers
Adsorption
Freshwater
Water monitoring

ABSTRACT

Saxitoxin (STX), the most widely distributed neurotoxin in marine waters and emerging cyanotoxin of concern in freshwaters, causes paralytic shellfish poisoning in humans upon consumption of contaminated shellfish. To allow for the efficient monitoring of this biotoxin, it is of high importance to find high-affinity materials for its adsorption. Herein, we report the design and synthesis of a covalent organic polymer for the efficient adsorption of STX. Two β-keto-enamine-based materials were prepared by self-assembly of 2,4,6-triformylphloroglucinol (Tp) with 2,5-diaminobenzoic acid (Pa-COOH) to give TpPa-COOH and with 2,5-diaminotoluene (Pa-CH_3) to give TpPa-CH_3. The carboxylic acid functionalized TpPa-COOH outperformed the methyl-bearing counterpart TpPa-CH_3 by an order of magnitude despite the higher long-range order and surface area of the latter. The

* Corresponding author.
** Corresponding author at: CINBIO, Universidade de Vigo, Department of Organic Chemistry, 36310 Vigo, Spain.
E-mail addresses: lauramaria.salonen@uvigo.es (L.M. Salonen), begona.espina@inl.int (B. Espiña).

https://doi.org/10.1016/j.jhazmat.2023.131247
Received 14 November 2022; Received in revised form 28 February 2023; Accepted 18 March 2023
Available online 22 March 2023

adsorption of STX by TpPa-COOH was fast with equilibrium reached within 1 h, and the Langmuir adsorption model gave a calculated maximum adsorption capacity, Q_m, of 5.69 mg g^{-1}, making this material the best reported adsorbent for this toxin. More importantly, the prepared TpPa-COOH also showed good reusability and high recovery rates for STX in natural freshwater, thereby highlighting the material as a good candidate for the extraction and pre-concentration of STX from aquatic environments.

1. Introduction

Saxitoxin (STX) is one of the most lethal biotoxins known with an oral LD_{50} value of 5.7 μg kg^{-1} for humans [27]. It is produced by cyanobacteria and dinoflagellates during (cyanobacterial) harmful algal blooms ((cyano)HABs), massive proliferation of dinoflagellates or cyanobacteria occurring with increasing frequency [17,24] in many fresh and marine waters due to climate change, water hypertrophication, and other effects stemming from human activity. STX and its documented 58 congeners, also known as paralytic shellfish toxins (PSTs), typically accumulate in filter-feeding bivalves and fishes [13,32,48], potentially leading to seafood poisoning outbreaks through the marine food chain [9,28]. In freshwaters, 15 STX-producing species of freshwater cyanobacteria have been identified and many surveillance studies indicate that STX-producing species are very commonly present in stagnant surface freshwater for drinking water or recreational uses [6]. Therefore, to prevent the occurrence of toxic outbreaks, it is of high importance to develop materials that allow for the efficient monitoring of these toxins [30,31].

For trace or ultra-trace analysis of organic contaminants from water samples, pretreatment and pre-concentration are often required prior to the quantification [56], and extraction techniques such as solid-phase extraction (SPE) [25], magnetic solid-phase extraction (MSPE) [11,18], and solid-phase microextraction (SPME)[4] have been developed for the concentration of STX. On the other hand, for saxitoxin removal, the most common method is based on adsorption using granular activated carbon (GAC) [34], although other adsorbent materials have also been reported, such as polymeric resins [36], mineral residues [3,12], oyster shell powder [26], and algal polysaccharide gels [29]. However, complicated implementation procedures, low specificity and adsorption capacity, and poor reusability of the reported adsorbents prompt the development of novel highly efficient and recyclable materials for STX adsorption [21,25,36].

Covalent organic polymers (COPs) are a class of porous organic nanomaterials constructed from organic units via covalent bonding [54,57]. Given their interesting characteristics such as light density, facile preparation, and high structural stability [1,40,50], COPs represent a promising class of adsorbent materials for water contaminants, and they have been reported to efficiently capture rare-earth elements [35,41], radioactive elements [54], organic dyes [15,22], and pesticides [14,20]. In addition, their chemical selectivity and adsorption capacity can be tailored through the incorporation of functionalities into the COP building units [49].

Herein, we report the synthesis of novel COP materials for the adsorption of STX from water. Two β-keto-enamine-based materials were obtained by reaction of 2,4,6-triformylphloroglucinol (Tp) with 2,5-diaminobenzoic acid (Pa-COOH) yielding TpPa-COOH and with 2,5-diaminotoluene (Pa-CH_3) yielding TpPa-CH_3. Carboxyl-functionalized TpPa-COOH was found to be > 10 times more efficient than the methylated control COP TpPa-CH_3. Further insight into the adsorption capacity of TpPa-COOH was gained through kinetics, adsorption isotherm, and equilibrium studies, and the material was found to feature adsorption capacity of over seven times higher than the best-performing reported adsorbents for STX. This, added to the reusability of the material and its high adsorption capacity for STX from natural water samples, establishes TpPa-COOH as a potential adsorbent for the monitoring of STX.

2. Experimental section

2.1. Synthesis of TpPa-COOH

TpPa-COOH was synthesized modifying a previously reported procedure [7]. Briefly, triformylphloroglucinol (Tp) (63 mg, 0.3 mmol, 1.0 equiv.), 2,5-diaminobenzoic acid (Pa-COOH) (136.9 mg, 0.9 mmol, 3.0 equiv.), and a mixture of dimethylacetamide (DMAc) and 1,4-dioxane (9:1, 3 mL) were added to a 10 mL ampoule, and the mixture was homogenized by ultrasonication at r.t. for 5 min. Then, aq. 6 M acetic acid (AcOH) (0.5 mL, 6.0 mmol, 10.0 equiv.) was added and the suspension was sonicated at r.t. for 5 min to obtain a homogenous dispersion. The reaction mixture was flash frozen in a liquid N_2 bath, the ampoule was sealed under vacuum, and heated in the oven at 120 ℃ for 3 d. After cooling to r.t., the solid was collected by filtration and washed sequentially with tetrahydrofuran (THF), *N*,*N*-dimethylformamide (DMF), ultrapure water, and acetone until a colorless filtrate was observed. The resulting solid was dried at 90 ℃ under nitrogen for 24 h to yield TpPa-COOH (89 mg, 77%) as dark-red-colored powder.

2.2. Synthesis of TpPa-CH_3

In a 10 mL ampoule, Tp (31.5 mg, 0.15 mmol, 1.0 equiv.) and 2,5-diaminotoluene (Pa-CH_3) (27.5 mg, 0.23 mmol, 1.5 equiv.) were dispersed in a mixture of mesitylene and 1,4-dioxane (1:1, 1.8 mL), and the mixture was homogenized by ultrasonication at r.t. for 10 min. Then, aq. 6 M acetic acid (0.25 mL, 1.5 mmol, 10.0 equiv.) was added and the suspension was sonicated at r.t. for 5 min to obtain a homogenous dispersion. The reaction mixture was flash frozen in a liquid N_2 bath, the ampoule was sealed under vacuum, and heated in the oven at 120 ℃ for 3 d. After cooling to r.t., the solid was collected by filtration and washed sequentially with THF, ultrapure water, and dichloromethane until a colorless filtrate was observed. The resulting solid was dried at 90 ℃ under nitrogen for 24 h to yield TpPa-CH_3 (41 mg, 81%) as red-brown powder.

2.3. Saxitoxin and decarbamoylsaxitoxin quantification

STX and decarbamoylsaxitoxin (dcSTX) quantification assays were conducted at a final volume of 200 μL in wells of flat-bottom opaque 96-well microplates following a literature-known procedure [52]. First, 50 μL of sample were added to the wells containing 12 μL of 10% aq. hydrogen peroxide and 126 μL aq. 1 M NaOH. The microplate was incubated for 2 min at 20 ℃ under constant shaking at 500 rpm. Then, 10.2 μL of glacial acetic acid were added to stop the oxidation reaction followed by a 5 min shaking (500 rpm) at 20 ℃. The fluorescence intensity of each well was measured using a multifunctional microplate reader at 340 nm excitation/395 nm emission, with the gain of 100 and 150.

2.4. Calibration curves for STX or dcSTX quantification

For the preparation of the calibration curve, STX or dcSTX stock solution was serially diluted to 5, 4, 3, 2, 1.5, 1, 0.5 μmol L^{-1} with ultrapure water, river water, lake water, or 0.1% aq. formic acid (Fig. S16—**20**). The calibration curves in the corresponding solvents were prepared using the software Origin 8.5, plotting the known concentration points of serial dilutions against the corresponding

fluorescence. Then, a non-linear pharmacology dose-response or linear fitting was applied.

2.5. Adsorption kinetics

A sample of 110 μL of a TpPa-COOH dispersion of 1 mg mL^{-1} in ultrapure water was spiked with a STX to give a final concentration of 10 μmol L^{-1}. Mixture was incubated (19 ℃, 1400 rpm) using Thermomixer Comfort Eppendorf MTP with a 1.5 mL block. After incubation of 1, 5, 10, 30 s, and 1, 5, 10, 30, 60, and 120 min, the collection of the supernatant was performed by filtration (Millex®-GN, hydrophilic Nylon membrane, 0.22 μm). Two-fold dilutions of the collected supernatants were quantified using the microplate method. Each time interval was performed in duplicate. The experimental kinetics were fitted with the pseudo-first-order and the pseudo-second-order kinetic models.

2.6. Adsorption isotherms at 19 ℃

Samples of 110 μL of a 1 mg mL^{-1} TpPa-COOH dispersion in ultrapure water were spiked with a STX concentration of 7, 10, 12, 15 and 30 μmol L^{-1}. For low STX concentrations, the volume of samples was increased to 1000 μL at 1 and 3 μmol L^{-1}, and 700 μL at 5 μmol L^{-1}, keeping the COP concentration constant. Mixtures were incubated at 19 ℃ for 45 min under constant shaking at 1400 rpm. The supernatant of the samples was collected by centrifugation (15,000 rpm, 19 ℃, 15 min). The collected supernatants were subjected to dilution or concentration by evaporation and then quantified for STX using the microplate method. Each sample was performed in duplicate.

Freundlich and Langmuir models were employed to analyze the equilibrium adsorption isotherm. Freundlich equation is as follows [51]:

$$\ln Q_e = \left(\frac{1}{n}\right)\ln Ce + \log K_F \quad (1)$$

where Q_e is the amount of adsorbate adsorbed onto the adsorbent in equilibrium (mg g^{-1}), C_e is the concentration of adsorbate in the equilibrium state (mg L^{-1}), and n and K_F are characteristic constants. K_F is an indicator of the adsorption capacity in the Freundlich theory. This constant is a parameter used to evaluate the strength of the adsorption process.

The maximum adsorption capacity (Q_m) can be calculated from the following equation:

$$Q_m = K_F C_0^{1/n} \quad (2)$$

where C_0 is the initial and highest concentration of the adsorbate in solution (mg L^{-1}).

The Langmuir equation is expressed as [16]:

$$\frac{C_e}{Q_e} = \left(\frac{1}{Q_m}\right)C_e + 1 \Big/ (Q_m K_L) \quad (3)$$

where K_L is the characteristic Langmuir model constant.

The main characteristics of the Langmuir isotherm can be expressed by a dimensionless constant described as the separation factor R_L, which is an important equilibrium parameter.

$$R_L = 1/(1 + K_L C_0) \quad (4)$$

where $R_L > 1$ indicates the adsorption to be unfavorable, $R_L = 1$ is linear, $0 < R_L < 1$ is favorable, and $R_L = 0$ is irreversible.

2.7. Adsorption and desorption assays

For adsorption, two replicates of 110 μL of a TpPa-COOH dispersion of 1 mg mL^{-1} in ultrapure water or river water were spiked with STX or dcSTX to give a final concentration of 10 μmol L^{-1}. Mixtures were incubated at 19 ℃ under constant shaking at 1400 rpm for 1 h. Then, the supernatants were collected by centrifugation (15,000 rpm, 19 ℃, 15 min) for STX quantification. For desorption, the precipitates from the adsorption assays were suspended in 150 μL of aqueous 0.1% formic acid, sonicated at r.t. for 10 min, and incubated for 12 h at 40 ℃ under constant shaking of 14,000 rpm. The samples were then centrifuged at 15,000 rpm for 15 min at 19 ℃, and the supernatants were analyzed for STX quantification.

2.8. COP recycling

The pellets obtained from the desorption assays were washed with ultrapure water (1 mL) under constant shaking at 1400 rpm for 30 min and collected by centrifugation (15,000 rpm, 19 ℃, 60 min). Then, the pellets were subjected to two adsorption−desorption−washing cycles, maintaining the COP and STX concentration. The recovery of STX for cycles 1–3 was compared and evaluated for the reusability of TpPa-COOH.

3. Results and discussion

3.1. Design, synthesis, and characterizations of COPs

STX is a tetrahydropurine compound containing two guanidinium groups with pK_a values of 11.5 and 8.24, respectively (Fig. 1**A**) [38]. At physiological pH, both moieties are positively charged [46]. In order to design an efficient adsorbent for STX, we considered the binding of the toxin to its natural targets. Saxiphilin, a high-affinity STX-binding protein found in bullfrogs, was found to bind STX through several carboxylic groups and cation−π interaction [23,55]. Interestingly, such STX recognition pattern is similar to that found in voltage-gated sodium (Na_V) channels [2,43], where the binding mechanism is mediated by electrostatic interactions between the five- and six-membered guanidinium rings of STX and carboxyl groups on the Na_V channels [8,44]. Therefore, we hypothesized that introduction of carboxylic acid moieties into the adsorbent material would allow for favorable interactions with STX through hydrogen bonds, whereas the aromatic moieties could engage in cation−π interactions.

To gain access to carboxylic-acid-bearing COP, we envisioned the synthesis of TpPa-COOH from Tp [5] and commercially available 2, 5-diaminobenzoic acid (Fig. 1**B**). After optimization of the conditions, the best results in terms of adsorption efficiency (vide infra) were obtained with the material synthesized in a mixture of DMAc/1,4-dioxane 9:1 (*v/v*) with 10.0 equiv. of 6 M AcOH as catalyst at 120 ℃ for 72 h. As a control material without the presence of carboxylic acid moieties, we prepared TpPa-CH_3 by reaction of Tp and 2,5-diaminotoluene in mesitylene/1,4-dioxane 1:1 (*v/v*) with 10.0 equiv. of 6 M AcOH as catalyst at 120 ℃ for 72 h. Fourier-transform infrared (FTIR) spectroscopy featured strong bands at 1614, 1552, and 1230 cm^{-1} for TpPa-COOH (Fig. 2**A**), which were assigned to the stretching vibrations of C═O, C═C, and C−N of the keto form of Tp, indicating the formation of the β-keto-enamine linkage [42]. The bands at 993 and 1691 cm^{-1} stem from O−H and C═O of the carboxylic group, respectively [19]. For TpPa-CH_3, the strong peaks at 1577 and 1228 cm^{-1} were attributed to the stretching of C═C and C−N in the keto form (Fig. 2**B**). Meanwhile, the attenuation of the C═O band (1635 cm^{-1}) and C−H band (2923 cm^{-1}) of Tp as well as the N−H stretching bands of diamine building block (3288 and 3377 cm^{-1} for TpPa-COOH; 3315 and 3396 cm^{-1} for TpPa-CH_3) indicates the complete consumption of the starting materials.

Small-angle X-ray scattering (SAXS) was employed to verify if the prepared materials present long-range order. Although TpPa-COOH was found to exhibit some crystalline character, with reflections at scattering vector $q = 3.4$ and 6.8 nm^{-1}, corresponding to distances $d = 1.85$, and 0.93 nm, as reported previously [7], disorder in the material is evident from the pattern (Fig. S1). Higher order, typical of covalent organic framework (COF) materials [33], was found in the case of TpPa-CH_3

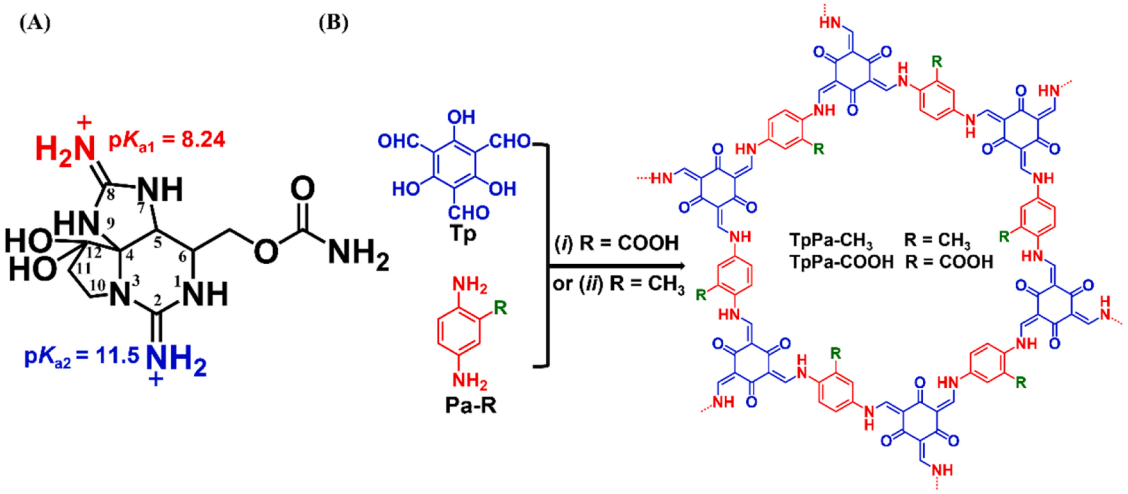

Fig. 1. Chemical structure of STX (A). Schematic illustration of the syntheses of TpPa-COOH and TpPa-CH_3 (B). (*i*) DMAc/1,4-dioxane 9:1, aq. 6 M AcOH; (*ii*) mesitylene/1,4-dioxane 1:1, aq. 6 M AcOH.

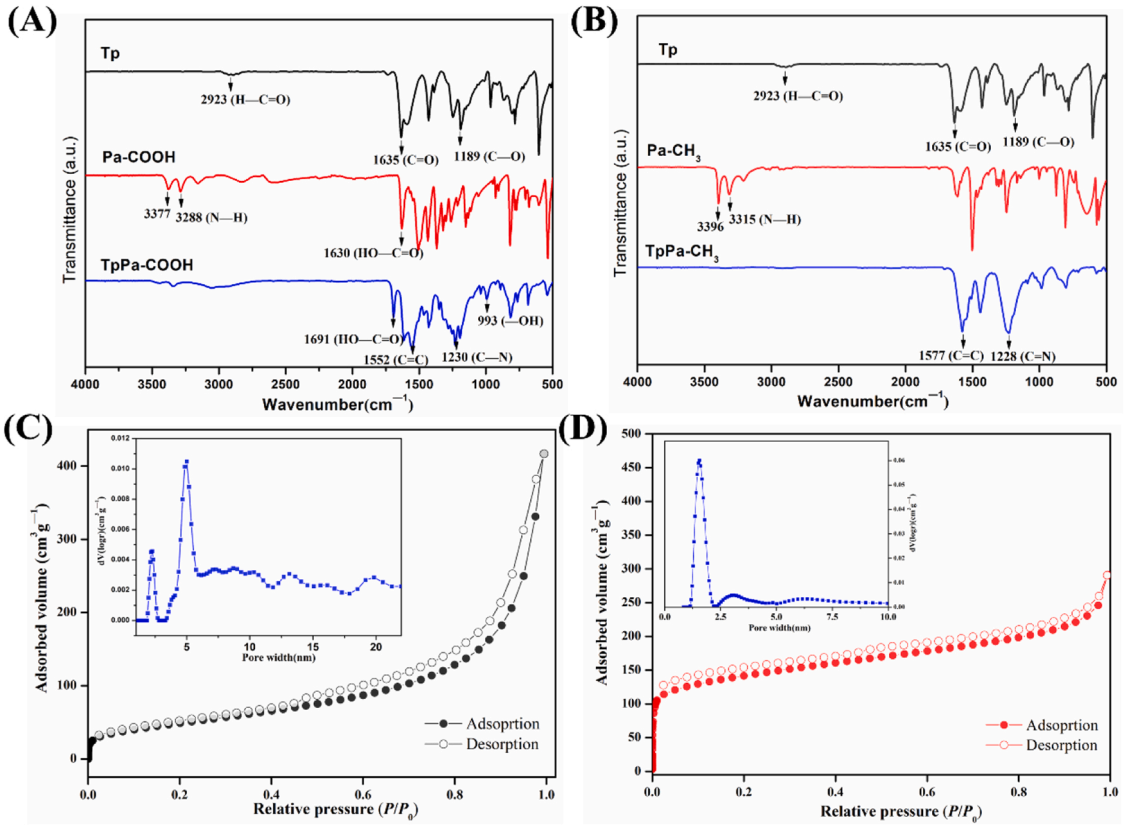

Fig. 2. FT-IR spectra of TpPa-COOH (A) and TpPa-CH_3 (B) overlaid with the corresponding monomers Tp, Pa-COOH, and Pa-CH_3. N_2 adsorption (filled spheres) and desorption (hollow spheres) isotherm profiles measured at 77 K of TpPa-COOH (C) and TpPa-CH_3 (D). (Insert) Pore size distribution calculated from quenched-solid density function theory (QSDFT).

(Fig. S2), with three main reflections at scattering vector $q = 3.25$, 5.50, and 18.9 nm^{-1}, corresponding to $d = 1.91$, 1.14, and 0.34 nm.

Nitrogen sorption measurements at 77 K showed type I sorption isotherms for both materials, indicating microporosity (Fig. 2**C** and **D and** Figs. S3 and 4), as revealed by the sharp increase in N_2 uptake at low pressures ($P/P_0 < 0.01$) [10]. Brunauer−Emmett−Teller (BET) surface areas of 177 and 531 $m^2\ g^{-1}$ were calculated for TpPa-COOH and TpPa-CH_3, respectively, the former in good agreement with the previous report [7]. The pore size distribution calculated using quenched-solid density functional theory (QSDFT) showed maxima at 2.3 and 5.0 nm as well as contributions from a mixture of larger pores for TpPa-COOH, further evidencing the lack of long-range order in the material. On the other hand, TpPa-CH_3 showed a more defined pore size at 1.6 nm.

Under nitrogen atmosphere (Fig. S9—**12**), thermogravimetric analysis (TGA) data exhibited the onset of weight losses for TpPa-COOH at 200 and 400 °C, attributed to decarboxylation and decomposition of the material, respectively [58]. Accordingly, TpPa-CH_3 only showed one weight loss starting at 315 °C. Scanning electron microscopy (SEM)

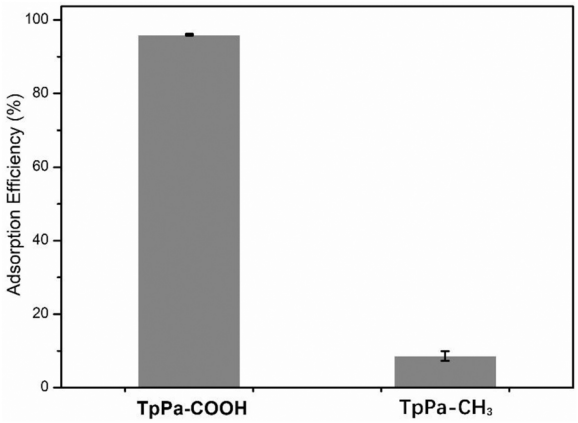

Fig. 3. Adsorption efficiency (%) of saxitoxin by TpPa-COOH and TpPa-CH_3 at an initial concentration of 5 μmol L^{-1} at C_0(COP)= 1 mg mL^{-1}. Experiment performed in duplicate at 19 ℃ in ultrapure water at pH 6–7. Error bars correspond to the standard deviation of the mean ($n = 2$).

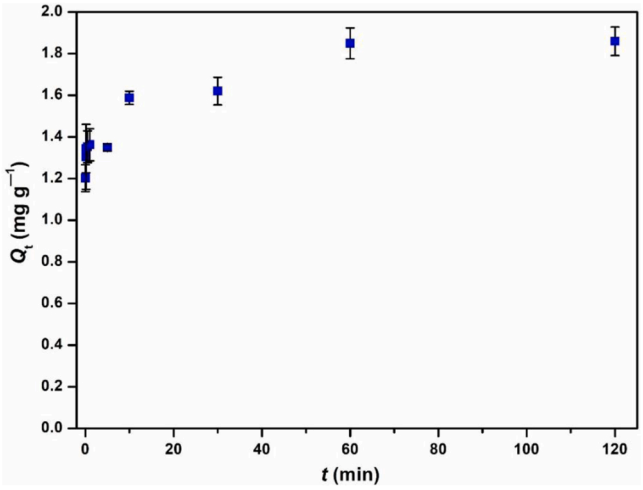

Fig. 4. STX adsorption kinetics at 10 μmol L^{-1} expressed as quantity adsorbed, Q_t (mg g^{-1}) as function of time, 1, 5, 10, 30 s, and 1, 5, 10, 30, 60, 120 min, performed in duplicate, at 19 ℃ in ultrapure water [C_0(COP) = 1 mg mL^{-1}]. Error bars correspond to the standard deviation of the mean ($n = 2$).

images showed TpPa-COOH as micron-sized particles and aggregates (Fig. S13), in agreement with the literature [7]. TpPa-CH_3 showed similar aggregations of numerous micrometer-ranged particles (Fig. S14).

3.2. Saxitoxin adsorption

To determine the adsorption efficiencies of TpPa-COOH and TpPa-CH_3 towards saxitoxin, adsorption tests were performed using COP dispersions of 1 mg mL^{-1} in ultrapure water spiked with a STX concentration of 5 μmol L^{-1}. After 4 h of incubation at 19 ℃ under constant shaking at 1400 rpm to ensure that equilibrium was reached, the supernatant of each sample was analyzed for STX quantification. As shown in Fig. 3, the adsorption efficiencies of saxitoxin by TpPa-COOH and TpPa-CH_3 were 96 ± 0.23% and 8.6 ± 1.31%, respectively, with TpPa-COOH outperforming TpPa-CH_3 by an order of magnitude despite having a smaller BET surface area and lower long-range order.

We postulate that the difference in adsorption efficiency between TpPa-COOH and TpPa-CH_3 could stem from the carboxylic acid moieties in TpPa-COOH, which may undergo favorable hydrogen-bonding interactions with the five- and six-membered guanidinium rings in STX, as seen in the binding of STX to saxiphilin and Na_V channels [8,55]. At the studied pH of 6–7, the guanidium moieties of STX, with pK_a values of 8.24 and 11.5 [37], are protonated, thus able to participate in such interactions. Of course, STX is highly polar in nature (log$D$[pH 7.4] = −5.49) [53], so the difference in the polarity of the materials could also play a role. However, both TpPa-COOH and TpPa-CH_3 exhibit similar water contact angle of 0° (Fig. S15).

3.3. Adsorption kinetics and test with analog dcSTX

As TpPa-COOH showed high adsorption efficiency to STX, we next carried out kinetic studies in ultrapure water at different contact times up to 2 h with a STX concentration of 10 μmol L^{-1}. This concentration was chosen since with 5 μmol L^{-1} the measured fluorescence value of the collected supernatants was below the linear range of the sigmoidal STX calibration curve for contact times over 10 min. As shown in Fig. 4, the equilibrium of adsorption was reached at 60 min, showing the adsorbed quantity q_t of 1.86 mg g^{-1} (t = 120 min, c(TpPa-COOH) = 1 mg mL^{-1}, c (STX) = 10 μmol L^{-1}). The experimental kinetic data were fitted with the pseudo-first-order and the pseudo-second-order kinetic models (Fig. S21—**22**), and the good fit of the latter indicated that this model is appropriate to describe the adsorption behavior of TpPa-COOH (Table S1), with the calculated Q_e of 1.82 mg g^{-1} identical to the experimental value. Additionally, we investigated the adsorption of a STX analog commonly found in natural waters, dcSTX. Very interestingly, TpPa-COOH was able to adsorb this analog with an even higher efficiency of 91%, reaching 4.1 mg g^{-1} of adsorption capacity experimentally.

3.4. Adsorption isotherm

The adsorption isotherm of STX with TpPa-COOH at 19 ℃ was obtained by plotting the amount absorbed in equilibrium, Q_e, against the remaining concentration of STX at equilibrium, C_e (Fig. 5). With increasing C_e, the equilibrium adsorption capacities rose linearly until reaching a transient saturation, and then continuing to rise. Langmuir and Freundlich isotherm models were employed to fit the experimental data (Fig. S23—**24**) and the isotherm parameters obtained by linear regression of the experimental values are listed in Table S2. The best fit of the data points was obtained with the Langmuir isotherm equation describing a monolayer adsorption process, with correlation coefficients

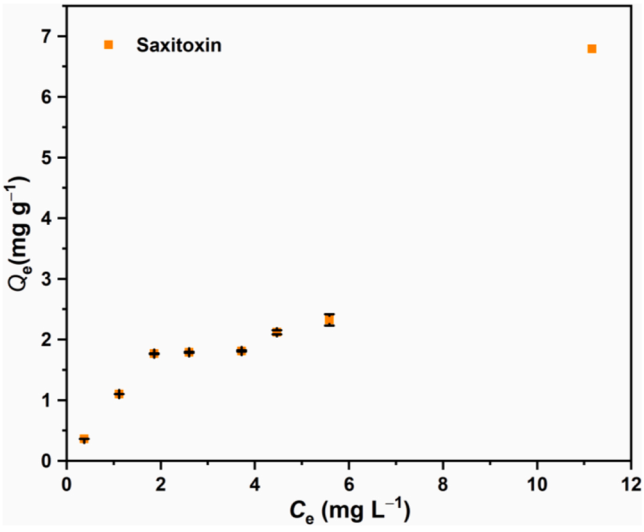

Fig. 5. Amount of STX adsorbed in equilibrium (60 min), Q_e (mg g^{-1}), as a function of STX concentration in equilibrium, C_e (mg L^{-1}), at 19 ℃ in ultrapure water [C_0(COP) = 1 mg mL^{-1}]. Error bars correspond to the standard deviation of the mean ($n = 2$).

close to 1. The values of constant K_L and separation factor R_L are 0.1852 and 0.3259, respectively, suggesting a favorable adsorption process of STX on TpPa-COOH ($0 < R_L < 1$). Therefore, the Langmuir isotherm model can more accurately describe the adsorption of STX by TpPa-COOH. The maximum adsorption capacity, Q_m, calculated from the adsorption isotherm was 5.69 mg g^{-1}, which matches very well the adsorption observed experimentally using 30 μM STX (6.79 mg g^{-1}). Importantly, with this value TpPa-COOH outperforms all reported adsorbents for the removal of STX from water (Table 1). In comparison, the STX adsorption capacity of TpPa-COOH is at least twice as high as those of previously reported materials, making it a potential candidate to be used as an efficient adsorbent for STX in the water.

3.5. Saxitoxin desorption and COP recycling

Regeneration of used adsorbents is crucial to reduce the costs of toxin removal and waste disposal, as well as for the adsorbent to be used as pre-concentration materials of STX for further analysis. To investigate the reusability of TpPa-COOH for the capture of STX, three consecutive adsorption−desorption cycles were performed with a STX concentration of 10 μmol L^{-1}. Prior to STX desorption measurements, we verified the elution ability of the alternative desorption solutions includinga mixture (pH 9–10) of methanol and ammonia in water, methanol/H_2O (1:1, *v/v*), and aqueous 0.1% formic acid (FA) solution. The 0.1% FA solution gave a much higher desorption efficiency than other candidates, suggesting that the enhanced polarity and acidity of the desorption solution is favorable for the elution of STX from TpPa-COOH, which could be due to protonation of the carboxylic groups of the COP. As shown in Fig. 6**A**, the adsorbed amount in equilibrium decreased merely from 1.85 to 1.81 mg g^{-1} in the first two cycles, and to 1.60 mg g^{-1} after three cycles. These results indicate that TpPa-COOH can maintain an acceptable performance for practical application at minimum of three consecutive uses. For desorption, recovery of adsorbed STX by TpPa-COOH for each individual cycle was determined as 86%, 83%, and 78%, respectively (Fig. 6**B**), providing a reliable toxin recovery. Furthermore, SAXS, FTIR, and N_2 sorption measurements of TpPa-COOH after three consecutive adsorption−desorption cycles confirmed that the adsorbent maintains its chemical and structural stability (Fig. S1 and Fig. S5—**8**), highlighting the durability of the material for this application.

Table 1
Comparison of the adsorption capacity of TpPa-COOH with reported adsorbents for STX adsorption.

Sorbent	Q_m (mg g^{-1})	Q_e (mg g^{-1})	T_{eq} (h)	Sorbent reuse	Ref.
SP700	0.000016	-	-	yes	[36]
CDP resins	0.0003	-	-	yes	[36]
m-Fe_3O_4@Carbon	0.061	-	1	-	[11]
Oyster shell powder	-	0.0004	72	-	[26]
Alginate gels	0.0007	0.00047	3	no	[29]
Semi-refined κ-carrageenan gels	0.0010	0.00048	3	no	[29]
Chitin	-	0.0005	72	-	[26]
Refined κ-carrageenan gel	0.0013	0.00067	3	no	[29]
CB1-MW-PAC	-	0.081	0.75	no	[39]
	-	0.076	1.25	no	[39]
WPH-PAC	-	2.43	24	no	[45]
GAC-DD	0.154 (exp.)	0.143	48	-	[47]
GAC-CB	0.415 (exp.)	0.203	48	-	[47]
GAC-AP	0.418 (exp.)	0.239	48	-	[47]
GAC-C8	2.095 (exp.)	0.252	48	-	[47]
TpPa-COOH	**5.69 (6.8 exp.)**	**1.82**	**1**	**yes**	**This work**

3.6. Extraction of saxitoxin by TpPa-COOH from natural waters

In order to probe the applicability of TpPa-COOH to adsorb STX from natural water, we collected a water sample from Cávado River, in Braga municipality, Portugal and a sample of water from Castiñeiras Lake, in Marin, Pontevedra, Spain. The pH of the river water sample was determined to be 6.89, very similar to the one from the lake, 6.86. Prior to adsorption experiments, the natural water samples were spiked with STX at concentrations of 5, 10, and 15 μmol L^{-1}. Although these concentrations far exceed actual contamination levels found in natural water, with the reported values generally being in the range of ng L^{-1} to μg L^{-1}, these experiments were carried out to allow for the comparison of the adsorption capacity of TpPa-COOH towards STX in natural water and ultrapure water. As shown in Fig. 7, the adsorption efficiency of STX by TpPa-COOH reached 99.7% (Test-1 river), 99.4% (Test-2 river) and 95% (Test-3 lake), all higher than the obtained value (94.9%) in ultrapure water. With increasing STX concentration, the adsorption efficiency showed a similar downward tendency in all water types, remaining below 50% at the highest concentration of 15 μmol L^{-1}. The adsorption capacities, Q_e, of TpPa-COOH for STX at 5 μmol L^{-1} was found to be 1.86 (Test-1 river), 1.85 (Test-2 river), 1.77 (Test-3 lake), and 1.77 mg g^{-1} (ultrapure water), respectively (Table S3).

In order to test the recovery of STX from the material after adsorption from natural water samples, the collected adsorbents obtained from the adsorption assay were re-suspended in 150 μL of aqueous 0.1% formic acid and incubated for 12 h under constant shaking of 1400 rpm. STX was recovered with good efficiency from the natural waters, presenting an adsorption recovery efficiency of 79% (Test-1 river), 73% (Test-2 river), and 59% (Test-3 lake), respectively, corresponding to 79%, 72%, and 56% recovery of the spiked amount (Table S4). In all cases, STX was efficiently recovered from TpPa-COOH (>59%), suggesting great applicability of TpPa-COOH for the extraction of STX from natural water for further analysis.

4. Conclusions

In summary, we have prepared carboxyl-functionalized TpPa-COOH COP with high adsorption efficiency towards STX and its analog, dcSTX. The material outperformed its methyl-bearing counterpart despite the higher long-range order and surface area of the latter, highlighting the importance of the carboxylic acid moieties in the adsorption. Adsorption experiments with TpPa-COOH revealed that adsorption equilibrium was reached within 60 min and calculated maximum adsorption capacity of the prepared material was 5.69 mg g^{-1}, outperforming all previously reported adsorbents for this toxin. Good reusability and high recovery efficiency of STX also from freshwater samples are further evidence of the great potential TpPa-COOH displays for saxitoxin extraction and pre-concentration for analytical applications.

Environmental Implications

Saxitoxin (STX), the most widely distributed neurotoxin in marine waters and emerging cyanotoxin of concern in freshwaters, causes paralytic shellfish poisoning in humans upon consumption of contaminated shellfish. In order to be able to detect low concentrations of STX in waters for analysis or early warning systems, efficient materials for its adsorption are needed. Here we report an adsorbent for STX based on a covalent organic polymer that, to the best of our knowledge, outperforms all the previously described ones, being able to reach high recoveries from natural waters and presenting a good reusability.

Supporting Information

Materials and methods, COP synthesis and characterization, details of the adsorption and desorption experiments, comparison of results with the literature (PDF).

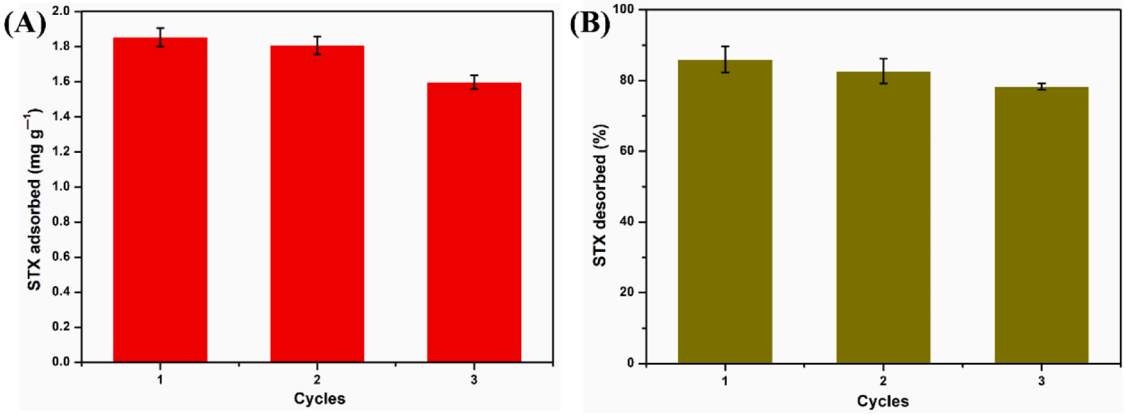

Fig. 6. Reusability of TpPa-COOH in consecutive cycles of STX adsorption/desorption at the initial concentration of 10 μmol L^{-1} (A). Quantification of the STX desorption efficiency (%) from TpPa-COOH using aqueous 0.1% formic acid after each adsorption/desorption cycle (B). Error bars correspond to the standard deviation of the mean ($n = 2$).

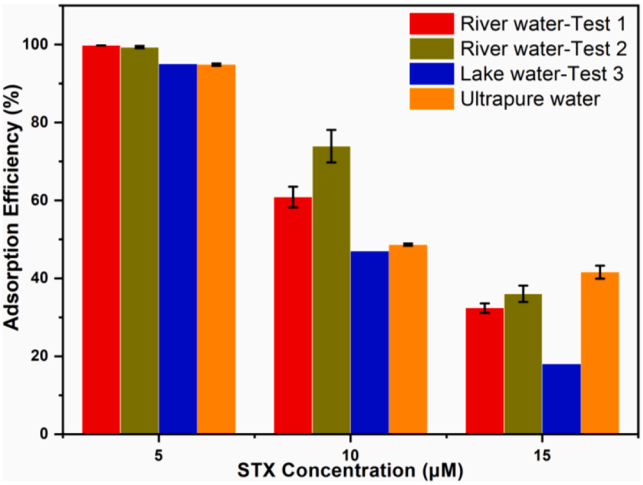

Fig. 7. Adsorption efficiency (%) of STX at concentrations of 5, 10, and 15 μmol L^{-1} by TpPa-COOH [C_0(COP) = 1 mg mL^{-1}] in river and lake water as well as ultrapure water. Error bars correspond to the standard deviation of the mean ($n = 2$).

Funding

Juliana Sousa is acknowledged for her help with the TGA measurements. Tianxing Wang gratefully acknowledges financial support from China Scholarship Council (CSC 202006150154). S.P.S.F. acknowledges the FCT – Fundação para a Ciência e Tecnologia for the Ph.D. scholarship SFRH/BD/131791/2017. L.M.S. acknowledges financial support from the Spanish Ministry of Science and Innovation through the Ramón y Cajal grant RYC2020-030414-I. This work has received funding from the project AIHABs (411), funded by Aquatic Pollutants, Water JPI, JPI Oceans, JPI AMR, the European Commission and FCT (Aquatic/0005/2020), as well as through the project Charm (PTDC/QUI-OUT/2095/2021) funded by the FCT.

Author Contributions

The manuscript was written through contributions of all authors. All authors have given approval to the final version of the manuscript.

CRediT authorship contribution statement

Tianxing Wang: Investigation, Writing – original draft. **Soraia P.S. Fernandes**: Investigation. **Joana Araújo**: Investigation. **Xiaoxi Li**: Supervision, Writing – reviewing. **Laura M. Salonen**: Data curation, Supervision, Writing – review & editing. **Begoña Espiña**: Conceptualization, Supervision, Writing – review & editing.

Declaration of Competing Interest

The authors declare the following financial interests/personal relationships which may be considered as potential competing interests: Tianxing Wang reports financial support by China Scholarship Council. Soraia P. S. Fernades reports financial support by Foundation for Science and Technology. Laura M. Salonen reports financial support by Spanish Ministry of Science. Begona Espina reports financial support by European Commission.

Data availability

Data will be made available on request.

Appendix A. Supporting information

Supplementary data associated with this article can be found in the online version at doi:10.1016/j.jhazmat.2023.131247.

References

[1] Beuerle, F., Gole, B., 2018. Covalent organic frameworks and cage compounds: design and applications of polymeric and discrete organic scaffolds. Angew Chem Int Ed 57, 4850–4878.
[2] Bricelj, V.M., Connell, L., Konoki, K., MacQuarrie, S.P., Scheuer, T., Catterall, W.A., Trainer, V.L., 2005. Sodium channel mutation leading to saxitoxin resistance in clams increases risk of PSP. Nature 434, 763–767.
[3] Burns, J.M., Hall, S., Ferry, J.L., 2009. The adsorption of saxitoxin to clays and sediments in fresh and saline waters. Water Res 43, 1899–1904.
[4] Chan, I.O.M., Lam, P.K.S., Cheung, R.H.Y., Lam, M.H.W., Wu, R.S.S., 2005. Application of solid phase microextraction in the determination of paralytic shellfish poisoning toxins. Analyst 130, 1524–1529.
[5] Chong, J.H., Sauer, M., Patrick, B.O., MacLachlan, M.J., 2003. Highly stable keto-enamine salicylideneanilines. Org Lett 5, 3823–3826.
[6] Christensen, V.G., Khan, E., 2020. Freshwater neurotoxins and concerns for human, animal, and ecosystem health: a review of anatoxin-a and saxitoxin. Sci Total Environ 736, 139515.
[7] Dong, B., Wang, W.J., Xi, S.C., Wang, D.Y., Wang, R., 2021. A carboxyl-functionalized covalent organic framework synthesized in a deep eutectic solvent for dye adsorption. Chem Eur J 27, 2692–2698.
[8] Durán-Riveroll, L.M., Cembella, A.D., Band-Schmidt, C.J., Bustillos-Guzmán, J.J., Correa-Basurto, J., 2016. Docking simulation of the binding interactions of saxitoxin analogs produced by the marine dinoflagellate Gymnodinium catenatum to the voltage-gated sodium channel NaV1. 4. Toxins (Basel) 8, 129.
[9] Farabegoli, F., Blanco, L., Rodríguez, L.P., Vieites, J.M., Cabado, A.G., 2018. Phycotoxins in marine shellfish: origin, occurrence and effects on humans. Mar Drugs 16, 188.

[10] Fu, Y., Wang, Z., Fu, X., Yan, J., Liu, C., Pan, C., et al., 2017. Acid/hydrazide-appended covalent triazine frameworks for low-pressure CO_2 capture: pre-designable or post-synthesis modification. J Mater Chem A 5, 21266–21274.
[11] González-Jartín, J.M., de Castro Alves, L., Alfonso, A., Piñeiro, Y., Vilar, S.Y., Rodríguez, I., Gomez, M.G., Osorio, Z.V., Sainz, M.J., Vieytes, M.R., 2020. Magnetic nanostructures for marine and freshwater toxins removal. Chemosphere 256, 127019.
[12] Guimarães Neto, J.O.A., Aguiar Jr, T.R., 2020. Evaluation of the efficiency of three different mineral adsorbents in the removal of pollutants in samples from a tropical spring in Northeastern Brazil. Water Environ Res 92, 1195–1207.
[13] Hackett, J.D., Wisecaver, J.H., Brosnahan, M.L., Kulis, D.M., Anderson, D.M., Bhattacharya, D., Plumley, F.G., Erdner, D.L., 2013. Evolution of saxitoxin synthesis in cyanobacteria and dinoflagellates. Mol Biol Evol 30, 70–78.
[14] Hao, L., Wang, Y., Wang, C., Wu, Q., Wang, Z., 2019. A magnetic covalent aromatic polymer as an efficient and recyclable adsorbent for phenylurea herbicides. Microchim Acta 186, 1–7.
[15] Jejurkar, V.P., Yashwantrao, G., Saha, S., 2020. Tröger's base functionalized recyclable porous covalent organic polymer (COP) for dye adsorption from water. New J Chem 44, 12331–12342.
[16] Langmuir, I., 1916. The constitution and fundamental properties of solids and liquids. Part I. Solids. J Am Chem Soc 38, 2221–2295.
[17] Lee, M., Shevliakova, E., Stock, C.A., Malyshev, S., Milly, P.C.D., 2019. Prominence of the tropics in the recent rise of global nitrogen pollution. Nat Commun 10, 1–11.
[18] Li, J., Zhu, J., Li, Y., Huang, T., Li, Y., 2020. l-Cysteine-modified magnetic microspheres for extraction and quantification of saxitoxin in rat plasma with liquid chromatography and tandem mass spectrometry. J Sep Sci 43, 2429–2435.
[19] Li, Y., Yang, C.-X., Qian, H.-L., Zhao, X., Yan, X.-P., 2019. Carboxyl-functionalized covalent organic frameworks for the adsorption and removal of triphenylmethane dyes. ACS Appl Nano Mater 2, 7290–7298.
[20] Liang, R., Peng, Y., Hu, Y., Li, G., 2019. A hybrid triazine-imine core-shell magnetic covalent organic polymer for analysis of pesticides in fruit samples by ultra high performance liquid chromatography with tandem mass spectrometry. J Sep Sci 42, 1432–1439.
[21] Liang, Y., Li, A., Chen, J., Tan, Z., Tong, M., Liu, Z., Qiu, J., Yu, R., 2022. Progress on the investigation and monitoring of marine phycotoxins in China. Harmful Algae 111, 102152.
[22] Liu, K., Huang, L., Shuai, Q., 2021. Solvent and catalyst free preparation of sulfonic acid functionalized magnetic covalent organic polymer as efficient adsorbent for malachite green removal. J Water Process Eng 43, 102306.
[23] Llewellyn, L.E., Moczydlowski, E.G., 1994. Characterization of saxitoxin binding to saxiphilin, a relative of the transferrin family that displays pH-dependent ligand binding. Biochemistry 33, 12312–12322.
[24] Lu, T., Zhang, Q., Lavoie, M., Zhu, Y., Ye, Y., Yang, J., Paerl, H.W., Qian, H., Zhu, Y.-G., 2019. The fungicide azoxystrobin promotes freshwater cyanobacterial dominance through altering competition. Microbiome 7, 1–13.
[25] MacKenzie, L.A., 2010. In situ passive solid-phase adsorption of micro-algal biotoxins as a monitoring tool. Curr Opin Biotechnol 21, 326–331.
[26] Melegari, S.P., Matias, W.G., 2012. Preliminary assessment of the performance of oyster shells and chitin materials as adsorbents in the removal of saxitoxin in aqueous solutions. Chem Cent J 6, 1–8.
[27] Micheli, L., Di Stefano, S., Moscone, D., Palleschi, G., Marini, S., Coletta, M., Draisci, R., 2002. Production of antibodies and development of highly sensitive formats of enzyme immunoassay for saxitoxin analysis. Anal Bioanal Chem 373, 678–684.
[28] Murray, S.A., Ruvindy, R., Kohli, G.S., Anderson, D.M., Brosnahan, M.L., 2019. Evaluation of sxtA and rDNA qPCR assays through monitoring of an inshore bloom of Alexandrium catenella Group 1. Sci Rep 9, 1–12.
[29] Olano, D.E.B., Salvador-Reyes, L.A., Montaño, M.N.E., Azanza, R.V., 2020. Sorption of paralytic shellfish toxins (PSTs) in algal polysaccharide gels. Algal. Research 45, 101655.
[30] Picardo, M., Núñez, O., Farré, M., 2020. Suspect and target screening of natural toxins in the Ter River catchment area in NE Spain and prioritisation by their toxicity. Toxins (Basel) 12, 752.
[31] Pitois, F., Fastner, J., Pagotto, C., Dechesne, M., 2018. Multi-toxin occurrences in ten french water resource reservoirs. Toxins (Basel) 10, 283.
[32] Pomati, F., Neilan, B.A., 2004. PCR-based positive hybridization to detect genomic diversity associated with bacterial secondary metabolism. Nucleic Acids Res 32 e7-e7.
[33] Qian, C., Liu, E.-C., Qi, Q.-Y., Xu, K., Jiang, G.-F., Zhao, X., 2018. A design strategy for the construction of 2D heteropore covalent organic frameworks based on the combination of C_{2v} and D_{3h} symmetric building blocks. Polym Chem 9, 279–283.
[34] Qiu, J., Fan, H., Liu, T., Liang, X., Meng, F., Quilliam, M.A., Li, A., 2018. Application of activated carbon to accelerate detoxification of paralytic shellfish toxins from mussels Mytilus galloprovincialis and scallops Chlamys farreri. Ecotoxicol Environ Saf 148, 402–409.
[35] Ravi, S., Puthiaraj, P., Yu, K., Ahn, W.-S., 2019. Porous covalent organic polymers comprising a phosphite skeleton for aqueous Nd (III) capture. ACS Appl Mater Interfaces 11, 11488–11497.
[36] Rodríguez, P., Alfonso, A., Turrell, E., Lacaze, J.-P., Botana, L.M., 2011. Study of solid phase adsorption of paralytic shellfish poisoning toxins (PSP) onto different resins. Harmful Algae 10, 447–455.
[37] Rogers, R.S., Rapoport, H., 1980. The pKa's of saxitoxin. J Am Chem Soc 102, 7335–7339.
[38] Rogers, R.S., Rapoport, H., 2002. The pKa's of saxitoxin. J Am Chem Soc 102, 7335–7339.
[39] Rorar, J., Garcia, L.D., Cutright, T., 2023. Removal of saxitoxin and anatoxin-a by PAC in the presence and absence of microcystin-LR and/or cyanobacterial cells. J Environ Sci 128, 161–170.
[40] Segura, J.L., Mancheño, M.J., Zamora, F., 2016. Covalent organic frameworks based on Schiff-base chemistry: synthesis, properties and potential applications. Chem Soc Rev 45, 5635–5671.
[41] Seo, Y., Hwang, Y., 2021. Prussian blue immobilized on covalent organic polymer-grafted granular activated carbon for cesium adsorption from water. J Environ Chem Eng 9, 105950.
[42] Sharath, Kandambeth, Arijit, Mallick, Binit, Lukose, Manoj, V., Mane, Thomas, 2012. Construction of crystalline 2D covalent organic frameworks with remarkable chemical (acid/base) stability via a combined reversible and irreversible route. J Am Chem Soc 134, 19524–19527.
[43] Shen, H., Li, Z., Jiang, Y., Pan, X., Wu, J., Cristofori-Armstrong, B., Smith, J.J., Chin, Y.K.Y., Lei, J., Zhou, Q., 2018. Structural basis for the modulation of voltage-gated sodium channels by animal toxins. Science 362, eaau2596.
[44] Shen, H., Liu, D., Wu, K., Lei, J., Yan, N., 2019. Structures of human Nav1. 7 channel in complex with auxiliary subunits and animal toxins. Science 363, 1303–1308.
[45] Shi, H., Ding, J., Timmons, T., Adams, C., 2012. pH effects on the adsorption of saxitoxin by powdered activated carbon. Harmful Algae 19, 61–67.
[46] Shimizu, Y., Hsu, C.P., Genenah, A., 1981. Structure of saxitoxin in solutions and stereochemistry of dihydrosaxitoxins. J Am Chem Soc 103, 605–609.
[47] Silva Buarque, N.M., de Brito Buarque, H.L., Capelo-Neto, J., 2015. Adsorption kinetics and diffusion of Saxitoxins on granular-activated carbon: influence of pore size distribution. J Water Supply: Res Technol 64, 344–353.
[48] Silva, M., Rey, V., Botana, A., Vasconcelos, V., Botana, L., 2016. Determination of gonyautoxin-4 in echinoderms and gastropod matrices by conversion to neosaxitoxin using 2-mercaptoethanol and post-column oxidation liquid chromatography with fluorescence detection. Toxins (Basel) 8, 11.
[49] Skorjanc, T., Shetty, D., Valant, M., 2021. Covalent organic polymers and frameworks for fluorescence-based sensors. ACS Sens.
[50] Sun, Q., Aguila, B., Perman, J., Earl, L.D., Abney, C.W., Cheng, Y., Wei, H., Nguyen, N., Wojtas, L., Ma, S., 2017. Postsynthetically modified covalent organic frameworks for efficient and effective mercury removal. J Am Chem Soc 139, 2786–2793.
[51] Unuabonah, E.I., Omorogie, M.O., Oladoja, N.A., 2019. Modeling in adsorption: fundamentals and applications. Composite Nanoadsorbents. Elsevier,, pp. 85–118.
[52] Vale, P., Ribeiro, I., Rodrigues, S.M., 2021. Workflow of the pre-chromatographic 'Lawrence'method for bivalves contaminated with Gymnodinium catenatum's paralytic shellfish poisoning toxins. Food Control 126, 108081.
[53] Wiese, M., D'Agostino, P.M., Mihali, T.K., Moffitt, M.C., Neilan, B.A., 2010. Neurotoxic alkaloids: saxitoxin and its analogs. Mar Drugs 8, 2185–2211.
[54] Yan, R.-H., Cui, W.-R., Zhang, C.-R., Li, X.-J., Huang, J., Jiang, W., Liang, R.-P., Qiu, J.-D., 2021. Bio-inspired hydroxylation imidazole linked covalent organic polymers for uranium extraction from aqueous phases. Chem Eng J 420, 129658.
[55] Yen, T.-J., Lolicato, M., Thomas-Tran, R., Du Bois, J., Minor Jr, D.L., 2019. Structure of the saxiphilin: saxitoxin (STX) complex reveals a convergent molecular recognition strategy for paralytic toxins. Sci Adv 5, eaax2650.
[56] Zhang, X., Ping, X., Zhuang, H., 2017. Ultrasensitive Nano-rt-iPCR for determination of polybrominated diphenyl ethers in natural samples. Sci Rep 7, 1–10.
[57] Zheng, J., Wahiduzzaman, M., Barpaga, D., Trump, B.A., Gutiérrez, O.Y., Thallapally, P., Ma, S., McGrail, B.P., Maurin, G., Motkuri, R.K., 2021. Porous covalent organic polymers for efficient fluorocarbon-based adsorption cooling. Angew Chem Int Ed 60, 18037–18043.
[58] Zheng, S.T., Zhang, J., Yang, G.Y., 2008. Designed synthesis of POM–organic frameworks from {Ni6PW9} building blocks under hydrothermal conditions. Angew Chem 120, 3973–3977.